

1990

The Utility of Three Multichannel Spectral Techniques for Multi-Piston Compressor Noise Source Identification

D. E. Brown
Purdue University

P. Sherman
Purdue University

Follow this and additional works at: <https://docs.lib.purdue.edu/icec>

Brown, D. E. and Sherman, P., "The Utility of Three Multichannel Spectral Techniques for Multi-Piston Compressor Noise Source Identification" (1990). *International Compressor Engineering Conference*. Paper 754.
<https://docs.lib.purdue.edu/icec/754>

This document has been made available through Purdue e-Pubs, a service of the Purdue University Libraries. Please contact epubs@purdue.edu for additional information.

Complete proceedings may be acquired in print and on CD-ROM directly from the Ray W. Herrick Laboratories at <https://engineering.purdue.edu/Herrick/Events/orderlit.html>

THE UTILITY OF THREE MULTICHANNEL SPECTRAL TECHNIQUES FOR MULTI-PISTON COMPRESSOR NOISE SOURCE IDENTIFICATION

Delores E Brown - Graduate Research Assistant, and
Peter J Sherman - Professor
Ray W. Herrick Laboratories
School of Mechanical Engineering
Purdue University

ABSTRACT

This work investigates the sources of noise from a 10-cylinder automotive air conditioning compressor using three multichannel spectral analysis techniques. Three transducers were incorporated into a compressor and their output signals as well as a sound pressure microphone signal were evaluated using these three spectral estimation techniques. First, a typical DFT method was utilized and the results and related discussion are in Section 3. An autoregressive multichannel spectrum estimation technique was applied second and is described in Section 4. Section 5 contains the results from the third spectrum estimation technique applied, a new point spectra by Foias *et. al* [FFS]. Results, comparisons, and conclusions on the utility of each of these methods are discussed in Section 6.

1. INTRODUCTION

Although the DFT approach can be very useful in recovering information about rotating mechanical systems [B], it also has some notable limitations. Specifically, if we consider the lagged-product correlation function

$$R_x(\tau) = \frac{\lim_{T \rightarrow \infty} 1}{T} \int_{-\tau/2}^{\tau/2} x(t) x(t + \tau) dt \quad (1)$$

then for $x(t)$ equal to a periodic burst of white noise, the DFT of {1} is simply a constant. For pulsed flow out of a cylinder $x(t)$ will be random, but not white. In this case the influence of the signal periodicity may be more evidenced in the spectrum, but since this type of signal is random, there will be no spectral lines. In contrast, a mechanically excited periodic waveform is much more likely to exhibit a line spectrum character. DFT methods are not well equipped to discern line spectrum from "near"-line spectrum. The autoregressive, AR, spectral method has been the most popular alternative to the DFT method. In spite of its potential for superior resolution however, it is more the less a continuous spectrum estimate. A new multichannel spectrum method by Foias, *et al.*[FFS] is designed for point spectrum identification. The goal of this work is to evaluate the potential utility of this method in comparison to DFT and AR methods for identifying the noise sources from an automotive compressor. The next section describes the compressor properties pertinent to spectral analysis. It also describes the measurement signals used in the analysis. Results obtained using the DFT method, the AR method, and the new point spectrum method [FFS] are

summarized in Sections 3, 4, and 5, respectively. Some discussion and conclusions are given in Section 6.

2. COMPRESSOR GEOMETRY, DYNAMICS, AND MEASUREMENT

The compressor is made of two aluminum halves bolted together, housing five dual-acting pistons equally spaced about a central shaft and driven by a swashplate, a concentric plate tilted at an angle. The piston spacing is such that no two are at top dead center at the same instant. Thus, the shaft sees periodic loading at a frequency of $10f_s$ where f_s is the shaft rotation frequency. The shaft has a resonance frequency at 615 Hz and the shell exhibits good transmission characteristics in that region (Fig.2d). Four transducer signals were collected: sound pressure from a single microphone located 24 inches in front of the compressor on the shaft centerline, shaft torque pulsation via two strain gages, rear discharge cylinder pressure, and vibration from an externally mounted accelerometer. Using a MassComp computer, 100 time records were collected using a 4kHz sampling frequency and 8192 points per record. This allowed a frequency resolution of 0.45 Hz. The nominal operating speed of the compressor was 1190 rpm, (20 Hz) throughout the testing. Admitting roughly 45 points per cycle of compressor operation, frequency resolution is much finer than that obtainable from a typical hard wired FFT analyzer, so that the significant effect of spectral "leakage" associated with the finite record size is reduced. This leakage was noticeable in all preliminary testing on several different compressors at different operating speeds using a hard wired FFT analyzer.

3. DFT SPECTRAL ANALYSIS

Single channel DFT spectral estimates were obtained by averaging DFT information for the 100 independent records. The sound pressure signal, Fig.1a, showed two regions of energy concentration, 600 Hz, and 1000 - 1300 Hz. The 600 Hz region appears most notably related to the spectral shape of the torque pulsation signal, Fig.1b. Because the discharge pressure, Fig.1c, in this region is similar to that in neighboring regions of lower sound pressure, it was concluded that the influence of the torque pulsation is effected through mechanical mechanisms. In the second region, again the discharge pressure indicates no direct relation in shape or spectral energy content. The shell accelerations appear to be significant in this region, which would tend to suggest that there are other internal mechanisms acting to excite the shell and influence the sound at these frequencies. Also note that the torque has no apparent relation in this region.

The simple coherence between each of the transducer signals and microphone signal was calculated, also using 100 averages. The coherence between the sound pressure signal and the torque pulsation signal in Fig. 2a, suggests a strong correlation at the shaft resonant frequency. The discharge pressure exhibits similar correlation to the sound pressure signal in this region, Fig.2b. But in light of the previous discussion of the actual autospectra energy content, it is not considered to be a major potential noise source mechanism. The correlation can be expected since the shaft vibration would be expected to generate periodic pulsations in the discharge pressure. The acceleration, Fig.2c, is also very coherent with the sound in this region and exhibits similar spectral shape to the sound signature. This suggests that

the shaft resonance may be causing vibrations in the shell through its mechanical links to the shell.

The coherence shows no relation in the torque signal in the 1000 Hz region. This region seems to be dominated by the acceleration and the discharge pressure. It would thus appear that the shell is being driven in this region by the discharge pressure because, even though the autospectra signals of the discharge pressure are not significant. Fig.2d shows the accelerometer response to shell impact (force input was relatively flat in the 0 - 1500 Hz range). The transmission properties of the shell are highest in the 600 Hz range and in the 1000 - 1300 Hz range. There is a dip in transmission around 700 Hz and the sound level reflects this. The single accelerometer location limits the significance of this single measurement because of the possibility of being on a node of a given excited mode, but several impact location and accelerometer locations were investigated and found to exhibit similar transmission regions. Fig.2d is included to show that in the regions of most concern in the sound signal, the shell exhibits good transmission characteristics.

4. MULTICHANNEL AUTOREGRESSIVE SPECTRAL ANALYSIS

The second spectral estimation technique applied to the 100 independent records was a low order autoregressive model. One reason this modelling technique is so frequently used is due to the sharp peaks exhibited in the spectra which are typically associated with high-resolution in spectral estimation.[M] The AR spectra were calculated using a Levinson algorithm (see [M] for discussion). The AR(20) spectra results for the 4 channels are given in the form of autospectra in Fig.3 and coherence in Fig.4. All of the autospectra reflect significant concentration of energy in the 600 Hz and 1000 Hz regions. This, combined with the strong coherence in these regions, shown in Fig.4 would suggest that all of the quantities, including shell vibration, discharge pressure, and shaft torsional vibration oscillations are strongly related to the sound pressure. This contradicts the conclusion from the DFT analysis. Specifically, it raises a question as to the influence of the discharge pressure, since its spectrum estimate, Fig.3c is most similar to that of the sound pressure signal, Fig.3a.

There are a number of possible explanations for the contradictory findings. They have to do with the way that the AR spectral estimate treats sinusoids (i.e. point spectrum). Specifically, the inclusion of point spectrum on any one channel will generally result in a "cross - talk" phenomenon to all other channels [M]. Also, being a continuous spectrum estimate, AR(n) spectra approach infinity at point spectrum frequencies. Hence no valid amplitude comparisons between channels is valid in this instance.

We now proceed to consider a new spectrum estimation method of [FFS] which is designed to identify point spectrum. Once identified one could return to Fig.3 and Fig.4 and re-evaluate the information within and between the four channels.

5. NEW MIXED SPECTRUM IDENTIFICATION TECHNIQUE

Even though the DFT method previously described, yields a significant amount of useful information in the autospectra and simple coherence analysis, there is no question that the signatures evaluated are very complex in that they contain highly periodic components due to the physical parameters which influence them (i.e. the 5 dual-acting pistons and related cylinders). As mentioned in the introduction, DFT analysis is not well suited for distinguishing periodic deterministic signatures such as impact responses from periodic random responses such as flow past a valve. Results of the last section also raise a question as to the utility of AR spectral analysis for rotating machinery. For this reason a recently developed mixed spectrum technique of [FFS] was considered. This method utilizes the well known multichannel autoregressive spectral matrices $\{AR_k(\omega)\}_{k=0}^n$ [M] to form the n^{th} order point spectrum estimate

$$ML_n(\omega) = \left(\sum_{k=0}^n AR_k(\omega)^{-1} \right)^{-1} \quad n = 0, 1, 2, \dots \quad (2)$$

Here ML refers to "maximum likelihood" as coined by Capon [C]. Because the AR spectra are computed recursively (2) is easily accommodated. The key property of the sequence of matrices (2) is that as n approaches infinity they converge (monotonically) to the point spectrum matrix. For further discussion of these properties see [FFS], [SL]. Noting that the $AR_k(\omega)$ spectra converge to dirac delta functions at point spectrum frequencies, and to continuous spectrum at other frequencies, would help explain apparent contradictions between the DFT and AR methods. Specifically, if the shaft torque pulsations induce even a small sinusoidal component in the discharge pressure, as it should, then the $AR(n)$ spectra at this oscillation frequency will approach infinity as the model order n approaches infinity.

The $ML_n(\omega)$ spectral matrix for the 4-channel measurement contains 4 eigenvalues at each ω . The number of channels containing point spectrum is deduced by the eigenvector information. Fig.5 shows the convergence properties of the eigenvalues of (2) as a function of model order. In the 600 Hz region λ_1 and λ_2 appear to converge. This suggests that only two of the 4 channels have truly periodic components at this frequency. The eigenvector information indicated that these channels correspond to the sound pressure and shaft vibration channel. Exactly, how the shaft vibration is transmitted to the sound pressure signal in this region is not clear. It is however clear that the discharge pressure and the shell vibration are not candidates for the transmission medium, since they exhibit no periodic tendencies. In the 1kHz region we again observe a periodicity on the sound pressure and shaft vibration channels at 1091 Hz, along with a notable lack of periodicity in the discharge pressure and shell acceleration signals. This is particularly interesting since the DFT analysis suggested no relation between the sound pressure signal and the shaft vibration, as evidenced by the coherence in Fig.2a, and by the level of shaft vibration in Fig.1b. This latter figure does include a small spike at 1084 Hz. The 7 Hz discrepancy between the number and the 1091 Hz frequency of convergence in Fig.5c could be real, or could be due to the well known bias which occurs in AR spectral analysis methods

[M]. If it is the latter, then one could speculate that the shaft is acting to sense the vibration of another noise source mechanism. At this point we cannot be certain. At 1300 Hz, we observe this same shaft vibration - sound pressure signal relation as we did at 1091 Hz.

6. CONCLUSIONS

This work has addressed the utility of three spectral methods for noise source identification involving rotating machinery. These included the usual DFT method, multichannel AR spectral analysis, and a new point spectrum method. The DFT method gave valuable information concerning possible relations between the sound pressure signal and various other measurement signals. Specifically, it suggested that the sound pressure signal most strongly related to the torque pulsation at 600 Hz and the shell vibration at 1kHz. It was unable to suggest more specific information associated with the noise source mechanisms. The AR spectral information was inconclusive at best, and suggested strong relations between the sound pressure signal and all other measurement signals. Based on the results of the last sections, it is believed that this is due to the point spectrum content involved. The ML spectra were very informative in this respect, and suggested that the shaft vibration and the sound pressure were both periodic in the spectral regions of concern. If one concludes that these periodicities are the major influences on the overall compressor noise level, then the analysis suggests that the discharge pressure and the shell acceleration are not likely noise source mechanisms. Rather one should pursue further investigations into elements connected with the shaft. This direction is supported by the observation that the highest sound pressure level is experienced from the clutch face.

7. REFERENCES

- [B] S Braun, Mechanical Signature Analysis, Theory and Applications, (Academic Press, 1986).
- [C] J Capon, High-resolution frequency-wavenumber spectrum analysis, Proc. IEEE, 57 (1969), 1408-18.
- [FFS] C Foias, A Frazho, and P Sherman, A new approach for determining the spectral data of multichannel harmonic signals in noise, Mathematics of Control, Signals and Systems, 3 (1), 34-43, (1990).
- [LS] D Lyon and P Sherman, "On the Performance of the Family of Multichannel ML Spectra for Recovery of Point Spectrum", IASTED International Symposium on Signal Processing and Digital Filtering, Lugano, Switzerland, June 18-21, 1990.
- [M] S Marple, Performance of multichannel autoregressive spectral estimators, Proceedings of the IEEE Inter Conf on Acoustics, Speech and Signal Processing, Tokyo, 1986, 197-200.
- [SL] P Sherman and K Lou, On the rate of convergence of the ML spectral estimate for identification of sinusoids in noise, Proceedings of the IEEE Inter Conf on Acoustics, Speech and Signal Processing, New York, 1988, 2380-3.

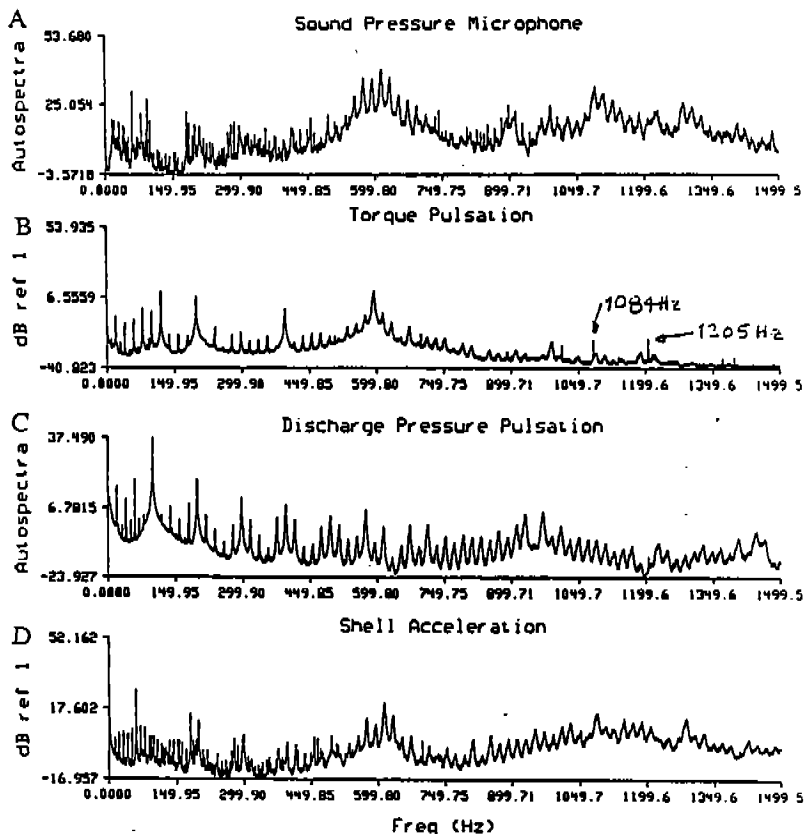
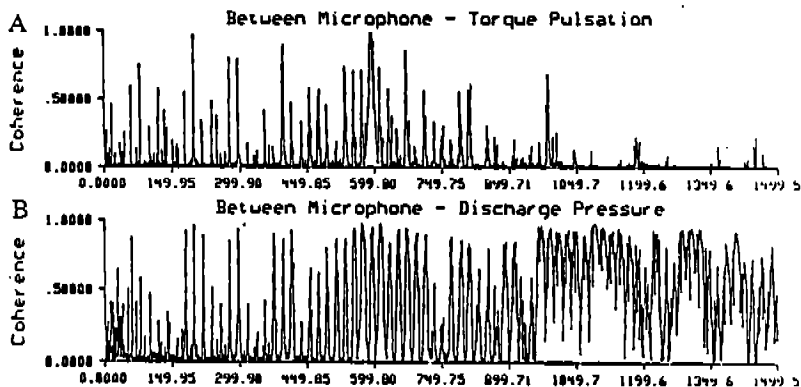


FIGURE 1. Autospectra for (a) Sound Pressure Microphone, (b) Torque Pulsation, (c) Discharge Pressure Pulsation, (d) Shell Acceleration. (all spectra dB ref 1)



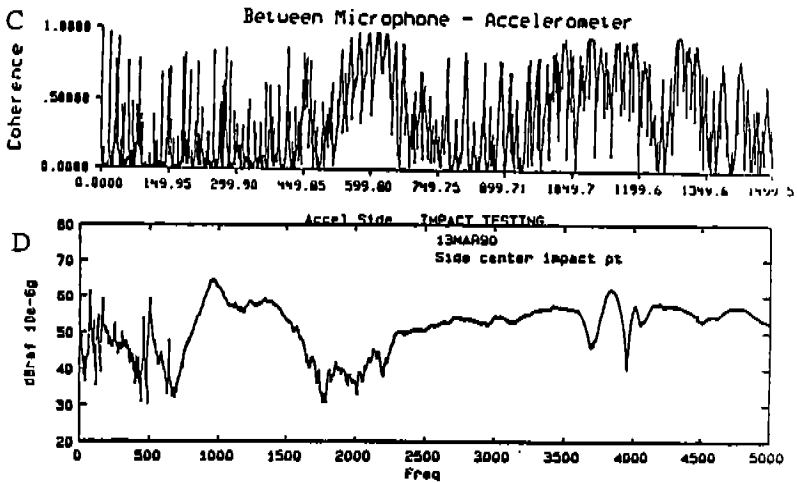


FIGURE 2. Coherence between (a) Sound Pressure signal and Torque Pulsation signal, (b) Sound and Discharge Pressure signal, (c) Sound and Shell Acceleration signal; (d) Shell Acceleration response to side shell impact. (all frequencies in Hz)

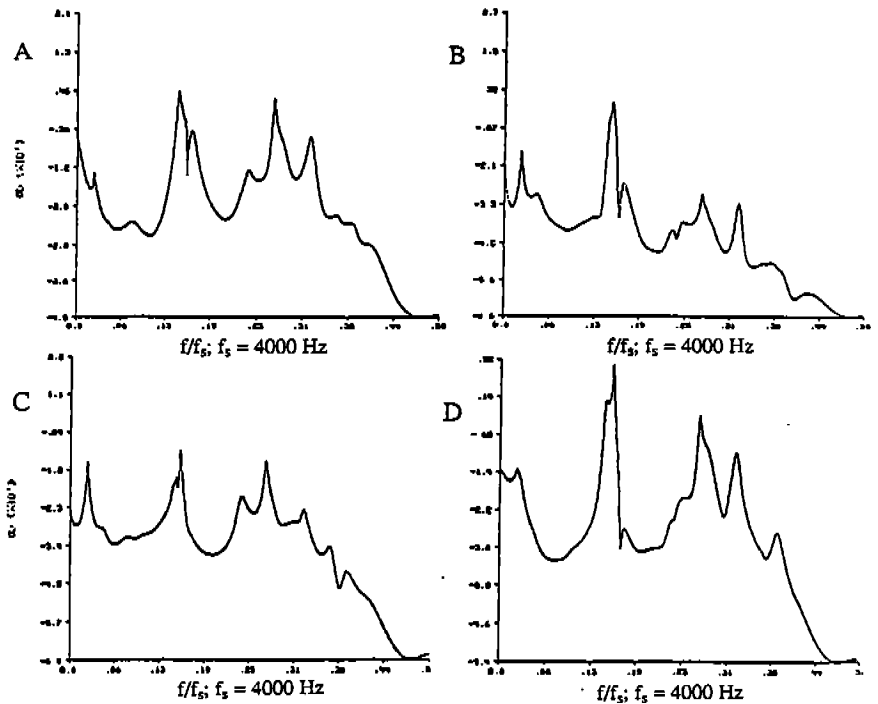


FIGURE 3. Autoregressive autospectra (a) Sound Pressure Microphone, (b) Torque Pulsation, (c) Discharge Pressure Pulsation, (d) Shell Acceleration.

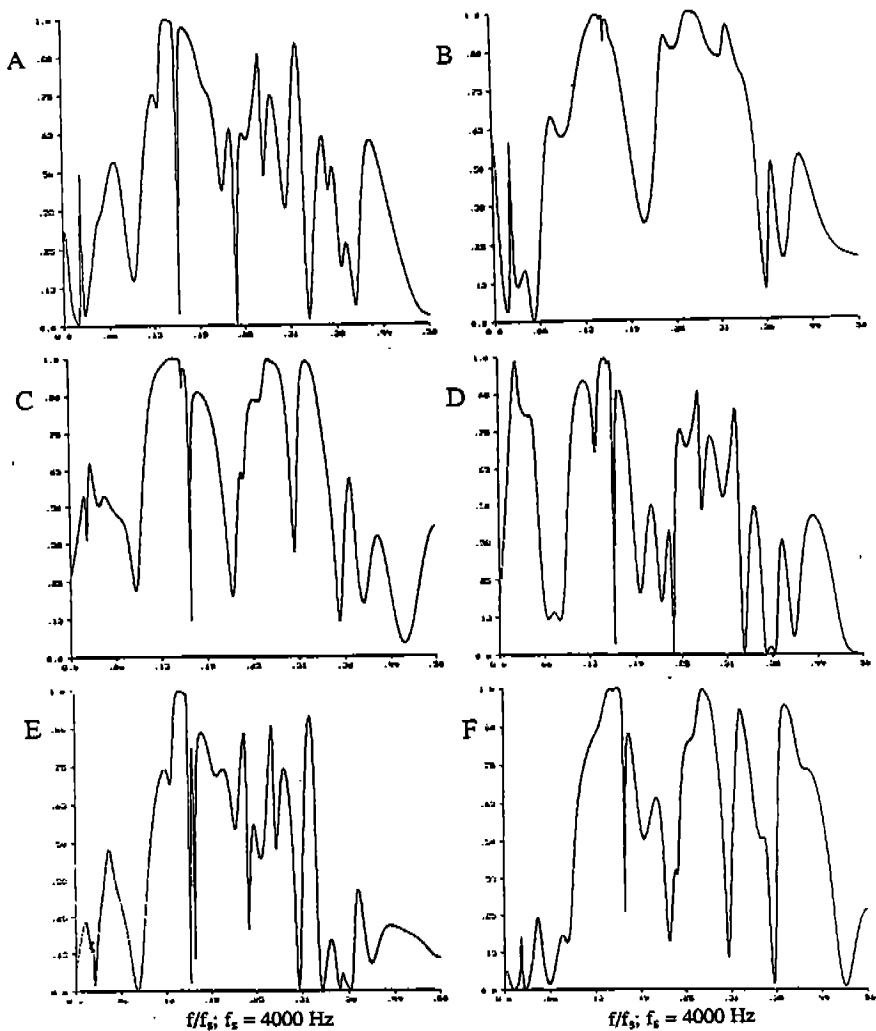


FIGURE 4. Autoregressive coherence between (a) Sound Pressure signal and Torque Pulsation signal, (b) Sound and Discharge Pressure signal, (c) Sound and Shell Acceleration signal; (d) Torque Pulsation and Discharge Pressure; (e) Torque Pulsation and Shell Acceleration; (f) Discharge Pressure and Shell Acceleration.

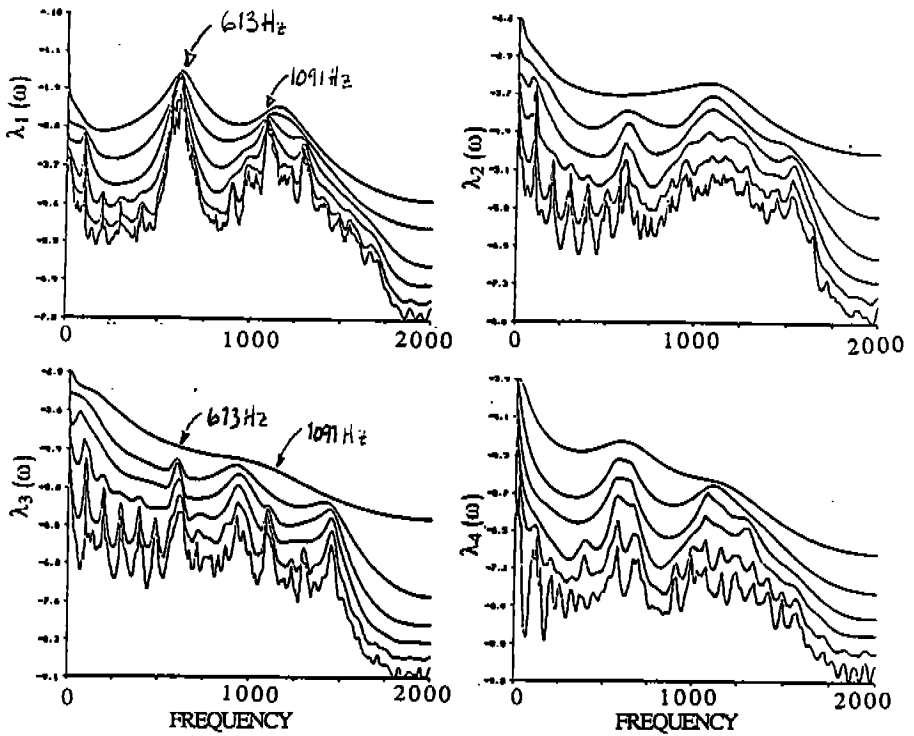


FIGURE 5. Eigenvalues $\lambda_1(\omega) \leq \lambda_2(\omega) \leq \lambda_3(\omega) \leq \lambda_4(\omega)$ associated with (2), for ML(160).

ACKNOWLEDGEMENT

This work was conducted with the financial support of the Climate Control Division of Ford Motor Company.